Separation Science and Technology
Publication details, including instructions for authors and subscription information:
http://www.informaworld.com/smpp/title~content=t713708471

A Model for Resistance Growth During Protein Microfiltration

Jia-Shyan Shiau[a]; Ching-Hsuan Tang[a]; Tong-Yo Lin[a]; Da-Ming Wang[a]
[a] Department of Chemical Engineering, National Taiwan University, Taipei, Taiwan

Online publication date: 20 February 2003

To cite this Article Shiau, Jia-Shyan , Tang, Ching-Hsuan , Lin, Tong-Yo and Wang, Da-Ming(2003) 'A Model for Resistance Growth During Protein Microfiltration', Separation Science and Technology, 38: 4, 917 — 932
To link to this Article: DOI: 10.1081/SS-120017634
URL: http://dx.doi.org/10.1081/SS-120017634

MARCEL DEKKER, INC. • 270 MADISON AVENUE • NEW YORK, NY 10016

SEPARATION SCIENCE AND TECHNOLOGY
Vol. 38, No. 4, pp. 917–932, 2003

A Model for Resistance Growth During Protein Microfiltration

Jia-Shyan Shiau, Ching-Hsuan Tang, Tong-Yo Lin, and Da-Ming Wang*

Department of Chemical Engineering, National Taiwan University, Taipei, Taiwan, ROC

ABSTRACT

Data reported in this study indicate that, in dead-end microfiltration of BSA solution, the compression of the deposited layer of protein aggregates on membranes governs the growth of filtration resistance in the late filtration period. Therefore, the mechanism of cake compression should be taken into account to describe the resistance growth during microfiltration. To develop a suitable model for the resistance growth due to compression, the time dependence of cake porosity was measured, and the relationship between specific cake resistance and cake porosity was determined. The results suggest that the time dependence of cake porosity can be described by the Voigt model and the relationship between porosity and specific resistance can be described by the Kozeny equation. With the Voigt model and the Kozeny equation, the resistance growth due to compression can be well modeled. By incorporating the compression

*Correspondence: Da-Ming Wang, Department of Chemical Engineering, National Taiwan University, Taipei, Taiwan 10617, ROC; Fax: +886-2-23623040; E-mail: daming@ccms.ntu.edu.tw.

DOI: 10.1081/SS-120017634 0149-6395 (Print); 1520-5754 (Online)

MARCEL DEKKER, INC. • 270 MADISON AVENUE • NEW YORK, NY 10016

model into the combined model of pore-blockage and cake-filtration, the resistance growth during microfiltration can be well described.

Key Words: Bovine serum albumin; Compression; Fouling; Microfiltration; Protein aggregates.

1. INTRODUCTION

A major problem often encountered in the application of protein filtration is the dramatic reduction in filtration flux caused by protein fouling.[1,2] It seems that severe fouling on microfiltration membrane should not occur because in such operations membrane pores are an order of magnitude larger than protein molecules; however, serious fouling is usually observed.[3] A lot of researches[4–8] have been performed to investigate how protein molecules, much smaller than membrane pores, can block the pores and cause dramatic flux decline.

One method to characterize the fouling mechanism is to analyze the resistance growth during filtration.[7] The filtration resistance (R) is defined as $R = \Delta P/(\mu J)$, where ΔP is the transmembrane pressure, μ represents the solution viscosity, and J denotes the filtration flux. A typical plot of R vs. filtration time for protein microfiltration is initially concave-up and followed by concave-down. The concave-up behavior can be described by pore-constriction or pore-blockage mechanism and the concave-down by cake-filtration mechanism.[5,6] Since the size of protein molecules is much smaller than the pore diameter of microfiltration membranes, the protein molecules are too small to directly block up the membrane pores. Therefore, it seems that pore-constriction is more suitable than pore-blockage to describe the initial fouling behavior in microfiltration. However, evidence has been obtained[9,10] showing that, although the nonaggregated protein is much smaller than the pores size of filtration membrane, the protein aggregates can be large enough to block up its pores and bring about dramatic flux decline. Several reports have verified the existence of aggregates in protein solution and investigated their role in membrane fouling.[11–18] Their results suggest that the initial fouling in protein microfiltration is caused by the blockage of membrane pores with the protein aggregates that were deposited on membrane surface, resulting in flux decline via a decrease in the area available for flow. The deposited protein aggregates can then serve as attachment sites for the subsequent deposition of the nonaggregated and aggregated protein, forming protein deposits (cake) over the initially blocked region.[10] By combining

the initial pore-blockage model and the subsequent cake-filtration model, the data of resistance growth can be well described.[19]

The applicability of the combined model of pore-blockage and cake-filtration is reexamined in the present work. The data to be reported indicate that the agreement between the combined model and the experimental measurement is limited to short filtration time. When the filtration time is long, the resistance growth in the late filtration period deviates severely from the prediction of the combined model. Evidence will be presented next to show that the deviation is due to not taking into account the compressibility of the deposited protein aggregates. A model is developed in the present work to describe the resistance growth due to cake compression. By combining this compression model with the models of pore-blockage and cake-filtration, a complete model is developed to give a thorough description of the mechanism of protein fouling in microfiltration.

2. THEORY

The growth rate of the amount of the deposited protein aggregates on membrane surface is proportional to the convective filtrate flux through that membrane. This relationship can be written as:

$$\frac{dm_p}{dt} = C_b f' J \tag{1}$$

where t represents the time, m_p the mass of the protein aggregates deposited on the membrane surface, C_b the protein concentration in the feed, f' the fraction of the protein that contributes to the growth of the deposit; i.e., the fraction of protein aggregates. With the definition of total filtration resistance (R_t), Eq. (1) can be rewritten as

$$\frac{dm_p}{dt} = C_b f' \frac{\Delta P}{\mu R_t} \tag{2}$$

The total filtration resistance can be expressed as $R_t = R_m + m_p \times R'$, where R_m is the membrane resistance and R' the specific resistance of the deposited protein. The membrane resistance is usually negligible compared with the resistance of the deposited protein. With the above information, Eq. (2) can be expressed as

$$\frac{dm_p}{dt} = C_b f' \frac{\Delta P}{\mu m_p R'} \tag{3}$$

Integration of Eq. (3) gives

$$\frac{m_p^2}{2} = \int_0^t \frac{C_b f' \Delta P}{\mu R'} dt \tag{4}$$

When the specific resistance of the deposited protein (R') is known, the deposited protein amount m_p can be calculated. The total cake resistance (resistance of the deposited protein, R_p) can then be obtained ($R_p = m_p R'$). If the deposited layer is incompressible R' is independent of time and can be treated as a constant to be determined by fitting the experimental data with the model. On the other hand, if the deposited layer is compressible a model that can describe the time dependence of R' is required to calculate R_p. How to obtain a model of R' will be discussed later.

When the membrane surface is covered with a deposited layer of protein aggregates, the total filtration resistance (R_t) equals to R_p if the membrane resistance is negligible. However, as mentioned by Ho and Zydney,[19] it takes time to develop a cake on the membrane surface. Hence, the above model of R_p cannot be used to describe the growth of total filtration resistance in the initial filtration period. By using the combined pore-blockage and cake-filtration model,[19] the above problem can be resolved. The procedure is described below. In the initial filtration period, the filtrate flux (J) through the fouled membrane equals the sum of the fluxes through the open and blocked pores and can be expressed as[19,20]:

$$J = \frac{\Delta P}{\mu R_m} \exp\left(-\frac{\alpha \Delta P C_b}{\mu R_m} t\right) + \frac{\Delta P}{\mu R_p}\left[1 - \exp\left(-\frac{\alpha \Delta P C_b}{\mu R_m} t\right)\right] \tag{5}$$

where α is the pore-blockage parameter. Substituting R_p into Eq. (5), the filtrate flux can be obtained. Then the total filtration resistance can be calculated by using $R_t = \Delta P/(\mu J)$.

3. EXPERIMENTAL

3.1 Materials

Bovine serum albumin (BSA) (Fraction V, Sigma Chemical Co.) was used as the model protein. BSA solutions were prepared by dissolving the powdered BSA in filtered phosphate-buffered solution. All BSA solutions were stored at 4°C and used within 24 hrs of preparation. The protein concentration was kept at 2 g/L and the pH was adjusted to 5.0

(close to the isoelectric point). The microfiltration membranes used were track-etched polycarbonate membranes (Millipore, average pore size: 0.2 μm).

3.2 Filtration Experiment

Dead-end microfiltration experiments were performed. A filtration chamber, with an effective area of 7.1 cm^2, was connected to a 2 L solution reservoir that was pressurized with air at 100 kPa. The weight of the filtrate was measured by a digital balance (A&D Co., HF 3000), which was connected to a personal computer. All experiments were conducted at room temperature.

3.3 SEM Analysis

Scanning electron microscope (Hitachi Co., JSM-6300) was used to study the surface characteristics of the fouled membranes. After filtration, the deposited layer on the fouled membrane was fixed by immersing the membrane in a 2 wt% glutaraldehyde solution for 30 mins. The membrane was then cleaned with buffer solution and dehydrated. The dehydration was conducted by rinsing the membrane repeatedly in ethanol aqueous solutions of successively increasing concentration: 50, 60, 70, 80, 90, and 99.5 wt%. The rinsing time was 10 mins for each level of concentration. The ethanol-treated membrane was then air-dried at 4°C. The dehydrated membranes were fractured in liquid nitrogen and coated with gold to prepare samples for SEM analysis.

3.4 In Situ Measurement of the Thickness of Protein Deposits on Membranes

A photointerrupt sensor (Sharp Co, GP2L22) was used to determine the thickness of the deposited layer (cake) on membrane surface during filtration. The photointerrupt sensor contains an infrared LED as emitter and a silicon transistor as collector. When an object near the sensor reflects the light from the emitter back into the collector, the reflective current can be well correlated with the distance between the object and the sensor. During microfiltration, the growth of the deposits would make the reflective surface (cake surface) move to the sensor, resulting in an increase in the reflective current. Hence, by measuring the change in the reflective current, the growth of cake thickness

during microfiltration can be determined. This method has been successfully applied to the measurement of cake thickness distribution in a cross-flow filtration system.[21] It was reported that the resolution of this technique could reach 10 μm. One can refer to Ref.[22] for more details of the design and the setup of this cake-thickness measuring system.

The sensor was calibrated by using a digital vernier with an accuracy of 10 μm. To calibrate the sensor, the sensor was tapped on the tail of the digital vernier. Filtration of 2 g/L BSA solution was performed for 2 hrs to produce a deposited protein layer (cake) on a membrane. The fouled membrane was then immersed in a bath of 2 g/L BSA solution. The sensor tapped on the vernier was placed in the BSA bath close to the fouled membrane. The distance between the sensor and the fouling layer can be adjusted in a scale of 10 μm by tuning the vernier. The distance between the fouling layer and the sensor can be well correlated with the reflective current, which was converted to voltage output by an electronic circuit. The calibration curve between the measured voltage and the distance between sensor and cake can then be obtained.

4. RESULTS AND DISCUSSION

4.1 Growth of Filtration Resistance During BSA Microfiltration

By measuring the filtration flux (J), the transmembrane pressure (ΔP), and the solution viscosity (μ), the total filtration resistance (R_t) can be calculated: $R_t = \Delta P/(\mu J)$. The filtration resistance is plotted versus the filtration time as shown in Fig. 1 for the filtration of a 2 g/L BSA solution. It can be seen that the resistance curve is concave-up initially and concave-down subsequently. It is known that the initial concave-up is consistent with the pore-blockage model, and the concave-down corresponds well to the cake-filtration model.[7] However, the resistance growth at longer filtration time does not obey the cake-filtration model: the resistance curve becomes concave-up again. The occurrence of the second concave-up region has been reported before,[7] but the associated mechanism is not yet clear.

Ho and Zydney[19] developed a combined pore-blockage and cake-filtration model to describe the protein fouling during microfiltration. By using their model the total filtration resistance can be calculated, and the results are depicted in Fig. 1. It can be seen clearly that the experimental data agree with the combined model in the first 6 hrs of filtration. However, after 6 hrs, the resistance curve is concave-up again and the model cannot predict such behavior. The discrepancy shown in Fig. 1 suggests that other fouling mechanisms besides pore-blockage and cake-filtration should be taken into

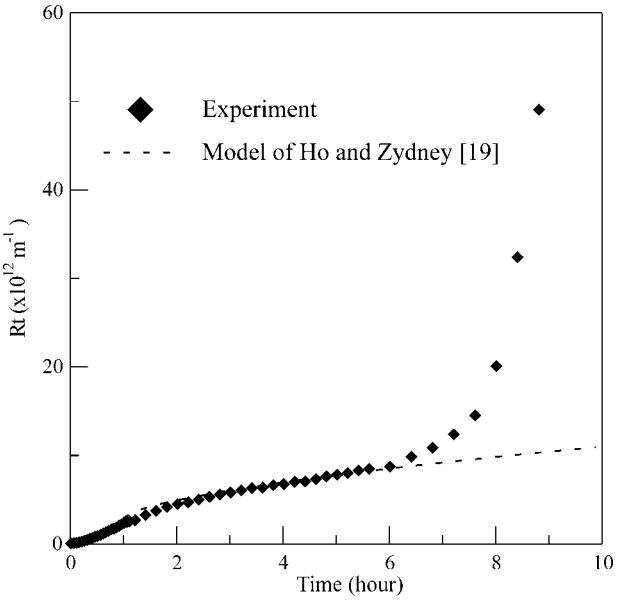

Figure 1. Resistance growth for the filtration of 2 g/L BSA solution at 1 atm and pH = 5.

account to give a thorough description of protein fouling during microfiltration.

Figure 2 presents the scanning electron micrographs of the surface morphology of the fouled membranes at different filtration time. The surface of the fouled membranes was covered with protein aggregates with a size of about 2 μm. Part of the membrane surface was covered after 5 mins of filtration. The area of the covered region increased with longer filtration time. The area available for flow is thus reduced accordingly. This observation supports that the initial flux decline is due to pore blockage. After about 1 hr of filtration, the whole membrane surface was covered with a layer of protein aggregates to form protein cake. After 6 hrs of filtration, a protein cake composed of protein aggregates can still be clearly observed. The above observations give a clear demonstration that the fouling during the first 6 hrs was caused by the mechanisms of pore-blockage and cake growth, providing grounds for the agreement of the experimental data and the model prediction shown in Fig. 1. However, after 9 hrs of filtration, dramatic change in the surface morphology was observed as demonstrated in Fig. 2(d). With 9 hrs of filtration, a uniform protein layer was formed on the membrane surface,

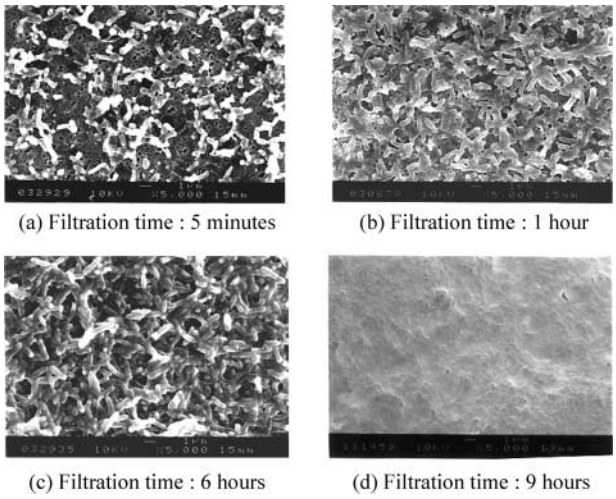

Figure 2. SEM analysis on the surface characteristics of the fouled membranes at different filtration time. Concentration: 2 g/L BSA, transmembrane pressure: 1 atm, pH = 5.

without any segregated protein aggregates. The results indicate that the BSA aggregates are deformable during filtration. After a long-time compression, the layer of segregated BSA aggregates [Fig. 2(c)] can deform to form a uniform dense layer [Fig. 2 (d)]. For more discussion on the deformation and compressibility of the cake of protein aggregates, one can refer to the work of Wang et al.[23] To model the resistance growth for a period ranging from 6 to 9 hrs, the effect of compression should be taken into account. Without taking this compression effect into account, the combined model[19] deviates severely from the experimental data as shown in Fig. 1. In the following, a model is developed to describe the effect of compression on resistance growth.

4.2 Change in Specific Resistance During Microfiltration

According to the results depicted in Fig. 2, the whole membrane surface was covered with a layer of protein aggregates after 1 hr of filtration. Hence, after 1 hr of filtration, the filtration resistance was governed by the cake property. To clarify how the cake property changes with filtration time, the specific cake resistance at different filtration time was investigated. In order to

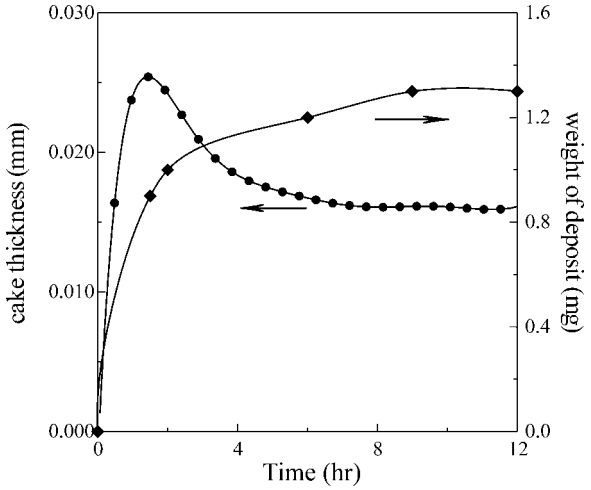

Figure 3. Time dependence of the mass of deposited protein and the cake thickness during microfiltration.

determine the specific cake resistance, the weight of the deposited protein on membrane was measured by direct weighing. The results are shown in Fig. 3. The amount of the deposited protein increases with time much faster in the initial period of filtration than in the late period. The growth rate of the amount of the deposited protein is proportional to the convective filtrate flux through that membrane. In the initial period the flux is high so that more protein aggregates can be brought to the membrane surface; on the other hand, in the late filtration period, the amount of protein increases slowly because of the low flux.

With the total resistance shown in Fig. 1 and the weight of deposited protein in Fig. 3, the specific resistance can be calculated and the results are shown in Fig. 4. When the filtration time is less than 6 hrs, the specific resistance is roughly constant; but when the filtration time is longer than 6 hrs, the specific resistance increases dramatically with filtration time. The results justify the usage of the combined model of Ho and Zydney[19] in which the specific cake resistance is assumed constant to calculate the total filtration resistance when the filtration time is less than 6 hrs. However, obviously it is not appropriate to assume the specific resistance constant when the filtration time is longer than 6 hrs, which can account for the deviation between model and data shown in Fig. 1.

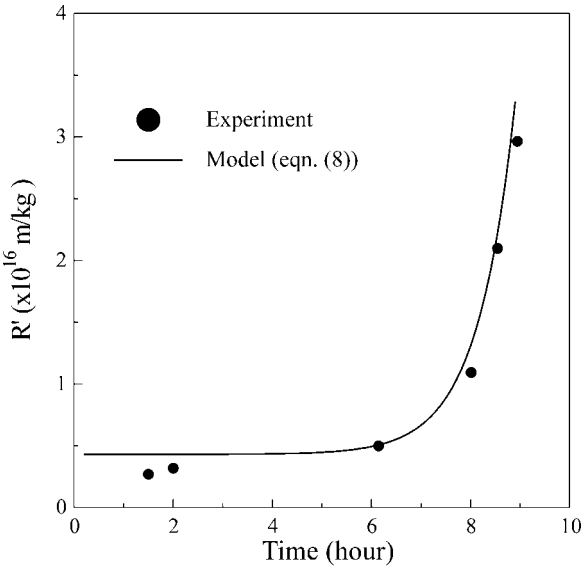

Figure 4. Growth of specific resistance during microfiltration.

4.3 Determination of the Average Cake Porosity

It is well known that the specific cake resistance is strongly related to the cake porosity. It should also be noted that the porosity distribution is not uniform for compressible (deformable) cake.[21] However, it is very difficult to measure the porosity distribution in protein cake. Therefore, in this study we only measured the average porosity and tried to correlate it with the specific cake resistance.

The volume of cake needs to be determined to calculate the average porosity. Hence, the cake thickness was measured, which can be used to calculate the cake volume. In this study, the thickness of protein cake was measured by using a photointerrupt sensor. The measurement procedure is described in Section 3.4. The cake thickness at different filtration time was measured and the results are depicted in Fig. 3. It can be seen that, in the initial period of filtration, the cake thickness increases with longer filtration time; while, in the late period, the thickness decreases over time. The result shown in Fig. 3 indicates that the dominant mechanism of fouling is different for the initial period and the late period of filtration.

In the initial period of filtration, the deposition of protein aggregates on the membrane surface and on the existing fouling layer (cake) dominates

the fouling behavior. Hence it is reasonable to observe that the cake thickness increases during filtration. In the late period of filtration, the flux becomes very low due to protein fouling, so that only a small amount of BSA aggregates is convected to the membrane surface. Thus, in the late period of filtration, the cake growth rate is low and the effect of compression governs the time dependence of cake thickness. Therefore, the cake thickness decreases with time. The decrease in cake thickness with filtration time clearly demonstrates that the cake of the deposited BSA aggregates is compressible and the compression of cake dominates the fouling behavior in the late period of filtration.

The mass of the deposited protein on membrane is shown in Fig. 3. The volume occupied by the deposited protein can be obtained by dividing the protein mass by the protein density. The volume of the deposited layer can be calculated with the measured thickness (Fig. 3) and the filtration area. After the volume of the deposited layer and that occupied by protein are known, the porosity can be calculated, and the results are shown in Fig. 5. The porosity decreases with increasing filtration time, indicating that the protein deforms more severely when it is subjected to the transmembrane pressure for a longer time. For a cake of deformable particles, it was suggested[21] that the change of

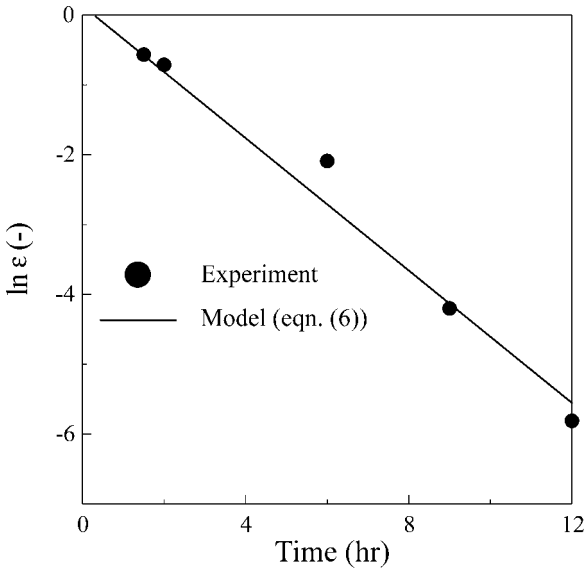

Figure 5. Time dependence of the porosity of the deposited layer during microfiltration.

cake porosity with time can be described by the Voigt model:

$$\frac{\varepsilon - \varepsilon_0}{\varepsilon_f - \varepsilon_0} = 1 - \exp\left(\frac{-t}{\tau}\right) \tag{6}$$

where ε_0 is the cake porosity before compression (t = 0), ε_f the cake porosity at equilibrium after compression ($t \rightarrow \infty$), and τ the retardation time constant. It was found that with $\varepsilon_0 = 0.774$, $\varepsilon_f = 0$, and $\tau = 8300$ s, the dependence of average porosity on time can be accurately described, as shown in Fig. 5. The results suggest that, although the theoretical basis is not yet clear, the Voight model can provide enough accuracy to describe the dynamic behavior of porosity of a deposited layer of protein aggregates when subjected to compression.

4.4 Relationship Between Specific Resistance and Average Porosity

For cake filtration, the Kozeny equation is widely used to describe the relationship between the specific cake resistance and the cake porosity:

$$R' = K \times \left(\frac{1 - \varepsilon}{\varepsilon^3}\right) \tag{7}$$

where K is the Kozeny constant and ε the porosity. Figure 6 presents the relationship between the specific cake resistance (Fig. 4) and $(1 - \varepsilon)/\varepsilon^3$. It can be seen that the specific resistance can be described by the Kozeny equation plus a constant:

$$R' = K \times \left(\frac{1 - \varepsilon}{\varepsilon^3}\right) + C \tag{8}$$

With $K = 1.26 \times 10^{11}\,\mathrm{m\,kg^{-1}}$ and $C = 4.5 \times 10^{15}\,\mathrm{m\,kg^{-1}}$, Eq. (8) can describe quite well the relationship between R' and ε, as shown in Fig. 4. The Kozeny equation has been widely used to describe the resistance of flow through porous media, but including a constant C in Eq. (8) requires justification. The agreement between experimental data and the model equation, shown in Fig. 4, justifies the necessity of including a constant in the Kozeny-like equation. According to the model of Ho and Zydney,[19] during microfiltration, membrane pores are firstly blocked by a layer of protein aggregates, on which further protein and aggregates can then deposit. We believe that the constant C in Eq. (8) accounts for the resistance of the first layer adjacent to the membrane pores, and the Kozeny part takes care of

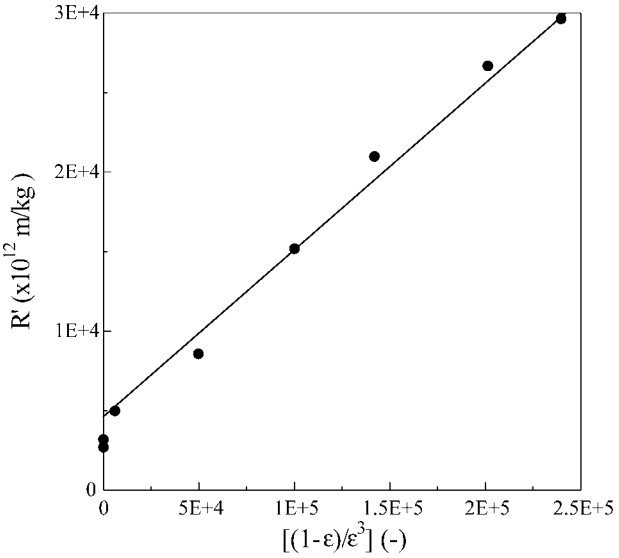

Figure 6. Relationship between the specific resistance (R′) and $(1-\varepsilon)/\varepsilon^3$.

further deposition. It should be noted that, although Eq. (8) can accurately describe the experimental data of specific resistance, it lacks solid theoretical fundamentals of using Eq. (8). The porosity distribution is in fact not uniform for compressible (deformable) cake.[21] Average porosity use might not be able to characterize the specific resistance, which should be sensitive to the porosity distribution. However, characterization of the porosity distribution is very difficult. Therefore, though Eq. (8) lacks solid theoretical basis, it is still used in the present work because of its simplicity and accuracy.

4.5 Combined Pore-Blockage, Cake-Filtration, and Cake-Compression Model

Once the dependence of R′ on t is known, the amount of deposited protein can be calculated by integration of Eq. (4). There is a parameter that still remains to be determined: f′, the fraction of protein aggregates. On the basis of Eq. (1), it can be derived that $m_p = C_b f' V$, where V is the volume of filtrate. By plotting m_p vs. V, a straight line with 0 intercept was obtained. With the slope of the straight line and Cb = 2 g/L, f′ can be determined to be 0.0008, on the same order of magnitude as that reported in the work of Ho and

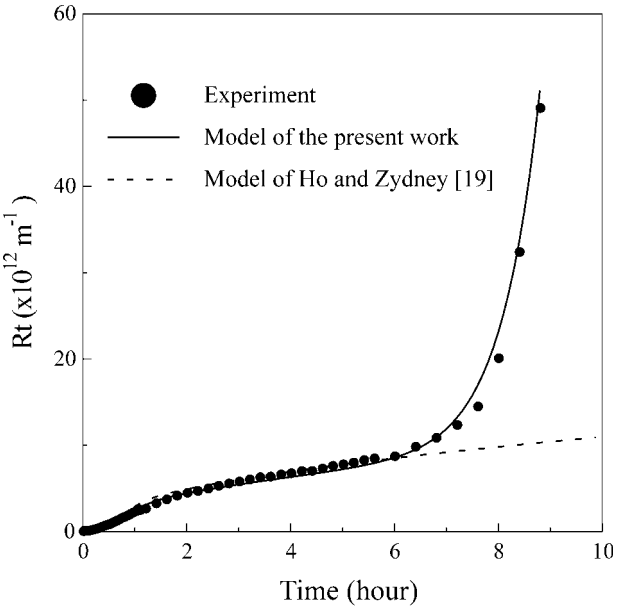

Figure 7. Comparison between the experimental data and model predictions for resistance growth during microfiltration.

Zydney[19] (0.0003). By substituting the $R'(t)$, obtained from Eqs. (6) and (8), into Eq. (4), m_p can be obtained. Then the cake resistance R_p can be calculated by multiplying m_p with R'. After the substitution of R_p into Eq. (5), the total filtration resistance can be obtained, and the results are depicted in Fig. 7. It can be seen clearly that the model can perfectly describe the growth of filtration resistance.

The results presented in Fig. 7 suggest that, to thoroughly describe the protein fouling in microfiltration, three mechanisms should be considered simultaneously: pore-blockage, cake-filtration, and cake compression. By incorporating a suitable compression model into the model developed by Ho and Zydney, the resistance growth during microfiltration can be well described.

CONCLUSION

The data presented indicate that, to describe the resistance growth during protein microfiltration, the mechanism of cake compression should be

taken into account. By using the Voigt model and the Kozeny equation, the resistance growth due to cake compression can be well modeled. By incorporating the compression model into the combined model of pore-blockage and cake-filtration, the resistance growth during microfiltration can be well described, suggesting that, to thoroughly describe the protein fouling in microfiltration, three mechanisms should be considered simultaneously: pore-blockage, cake-filtration, and cake compression.

ACKNOWLEDGMENTS

The authors wish to sincerely thank the National Science Council of Taiwan, ROC (NSC 90-2214-E-002-026) for rendering financial support for this project. In addition, we appreciate the kind help on performing SEM analysis from Miss Su-Jen Ji and Mr. Liang-Ping Lin, in the advanced instrument center, National Taiwan University.

REFERENCES

1. Zeman, L.J.; Zydney, A.L. *Microfiltration and Ultrafiltration: Principle and Application*; Marcel Dekker: New York, 1996.
2. Marshall, A.D.; Munro, P.A.; Tragardh, G. The effect of protein fouling in microfiltration and ultrafiltration on permeate flux, protein retention and selectivity: a literature review. Desalination **1993**, *91*, 65.
3. Belfort, G.; Davis, R.H.; Zydney, A.L. The behavior of suspensions and macromolecular solutions in crossflow microfiltration. J. Membr. Sci. **1994**, *96*, 1.
4. Hermans, P.H.; Bredee, H.L. Zur kenntnis der filtrationsgesetze. Rec. Trav. Chim. Des Pays-Bas **1935**, *54*, 680.
5. Hermia, J. Constant pressure blocking filtration laws—application to power-law non-Newtonian fluids. Trans. Inst. Chem. Eng. **1982**, *60*, 183.
6. Iritani, E.; Mukai, Y.; Tanaka, Y.; Murase, T. Flux decline behavior in deadend microfiltration of protein solutions. J. Membr. Sci. **1995**, *103*, 181.
7. Tracy, E.M.; Davis, R.H. Protein fouling and track-etched polycarbonate microfiltration membranes. J. Colloid Interface Sci. **1994**, *167*, 104.
8. Bowen, W.R.; Calvo, J.I.; Hernandez, A. Steps of membrane blocking in flux decline during protein microfiltration. J. Membr. Sci. **1995**, *101*, 53.
9. Kelly, S.T.; Opong, W.S.; Zydney, A.L. The influence of protein aggregates on the fouling of microfiltration membranes during stirred cell filtration. J. Membr. Sci. **1993**, *80*, 175.

10. Kelly, S.T.; Zydney, A.L. Mechanisms for BSA fouling during microfiltration. J. Membr. Sci. **1995**, *107*, 115.
11. Fane, A.G.; Fell, C.J.D.; Waters, A.G. Ultrafiltration of protein solutions through partially permeable membranes—the effect of adsorption and solution environment. J. Membr. Sci. **1983**, *16*, 211.
12. Chandavarkar, A.S. Dynamics of fouling of micrporous membranes by proteins. Ph.D. Thesis, Massachusetts Institute of Technology, 1990.
13. Kim, K.J.; Fane, A.G.; Fell, C.J.D.; Joy, D.C. Fouling mechanisms of membranes during protein ultrafiltration. J. Membr. Sci. **1992**, *68*, 79.
14. Kim, K.J.; Chen, V.; Fane, A.G. Some factors determining protein aggregation during ultrafiltration. Biotechnol. Bioeng. **1993**, *42*, 260.
15. Kelly, S.T.; Zydney, A.L. Effects of intermolecular thio-disulfide interchange reactions on BSA fouling during microfiltration. Biotechnol. Bioeng. **1994**, *44*, 972.
16. Bowen, W.R.; Gan, Q. Properties of microfiltration membranes—flux loss during constant pressure permeation of bovine serum albumin. Biotechnol. Bioeng. **1991**, *38*, 688.
17. Meireles, M.; Aimar, P.; Sanchez, V. Albumin denaturation during ultrafiltration: effects of operating conditions and consequences on membrane fouling. Biotechnol. Bioeng. **1991**, *38*, 528.
18. Ho, C.C.; Zydney, A.L. Effect of membrane morphology on the initial rate of protein fouling during microfiltration. J. Membr. Sci. **1999**, *155*, 261.
19. Ho, C.C.; Zydney, A.L. A combined pore blockage and cake filtration model for protein fouling during microfiltration. J. Colloid Interface Sci. **2000**, *232*, 389.
20. Wei, Y.; Aleksandra, K.; Zydney, A.L. Analysis of humic acid fouling during microfiltration using a pore blockage-cake filtration model. J. Membr. Sci. **2002**, *198*, 51.
21. Lu, W.M.; Tung, K.L.; Pan, C.S.; Hwang, K.J. Crossflow microfiltration of mono-dispersed deformable particle suspension. J. Membr. Sci. **2002**, *198*, 225.
22. Tung, K.L.; Wang, S.; Lu, W.M.; Pan, C.H. In situ measurement of cake thickness distribution by a photointerrup sensor. J. Membr. Sci. **2001**, *190*, 57.
23. Wang, D.-M.; Tang, C.-H.; Shiau, J.-S.; Lin, T.-Y. Role of the compression of protein aggregates in the development of filtration resistance during microfiltration. J. Membr. Sci., submitted for publication.